Spontaneously Modulated Spin Textures in a Dipolar Spinor Bose-Einstein Condensate

M. Vengalattore,[1] S. R. Leslie,[1] J. Guzman,[1] and D. M. Stamper-Kurn[1,2]

[1]*Department of Physics, University of California, Berkeley, California 94720, USA*
[2]*Materials Sciences Division, Lawrence Berkeley National Laboratory, Berkeley, California 94720, USA*

Helical spin textures in a ^{87}Rb $F = 1$ spinor Bose-Einstein condensate are found to decay spontaneously toward a spatially modulated structure of spin domains. The formation of this modulated phase is ascribed to magnetic dipolar interactions that energetically favor the short-wavelength domains over the long-wavelength spin helix. The reduction of dipolar interactions by a sequence of rf pulses results in a suppression of the modulated phase, thereby confirming the role of dipolar interactions in this process. This study demonstrates the significance of magnetic dipole interactions in degenerate ^{87}Rb $F = 1$ spinor gases.

　　　　PACS numbers: 05.30.Jp, 03.75.Mn, 75.45.+j, 75.50.Mm

In a wide range of materials, the competition between short- and long-range interactions leads to a rich landscape of spatially modulated phases arising both in equilibrium and as instabilities in nonequilibrated systems [1,2]. In classically ordered systems such as magnetic thin films [3] and ferrofluids [4], short-range ferromagnetic interactions are commonly frustrated by the long-range, anisotropic magnetic dipolar interaction, rendering homogeneously magnetized systems intrinsically unstable to various morphologies of magnetic domains [5]. Long-range interactions are also key ingredients in many models of strongly correlated electronic systems [6] and frustrated quantum magnets [7].

In light of their relevance in materials science, strong dipole interactions have been discussed as an important tool for studies of many-body physics using quantum gases of atoms and molecules, offering the means for quantum computation [8], simulations of quantum magnetism [9] and the realization of supersolid or crystalline phases [10,11]. However, in most ultracold atomic gases, the magnetic dipolar interaction is dwarfed by the contact (*s*-wave) interaction. Hence, experimental efforts to attain dipolar quantum gases have focused on nonalkali atoms, notably ^{52}Cr with its large magnetic moment [12], and on polar molecules [13].

In this Letter, we demonstrate that magnetic dipole interactions play a critical role in the behavior of a quantum degenerate $F = 1$ spinor Bose gas of ^{87}Rb. In this quantum fluid, *s*-wave collisions yield both a spin-independent and a spin-dependent contact interaction [14,15], with strengths proportional to $\bar{a} = (2a_2 + a_0)/3$ and $\Delta a = (a_2 - a_0)/3$, respectively, where the scattering length a_F describes collisions between particles of total spin F. In ^{87}Rb, with $a_0(a_2) = 5.39(5.31)$ nm, the spin-dependent contact interaction is far weaker than the spin-independent one; nevertheless, it is a critical determinant of the magnetic properties of degenerate $F = 1$ ^{87}Rb gases [16–18]. The magnetic dipole interaction strength may be parameterized similarly by a length $a_d = \mu_0 g_F^2 \mu_B^2 m/ (12\pi\hbar^2)$, where μ_0 is the permeability of vacuum, $g_F =$

1/2 the gyromagnetic ratio, μ_B the Bohr magneton and m the atomic mass [19]. Given $a_d/\Delta a = 0.4$, the $F = 1$ spinor Bose gas of ^{87}Rb is an essentially dipolar quantum fluid [20].

In our study, the influence of dipolar interactions on the spinor gas is evidenced by the spontaneous dissolution of deliberately imposed long-wavelength helical spin textures, in favor of a finely modulated pattern of spin domains. We ascribe the emergence of this modulated phase to the magnetic dipole energy that disfavors the homogenously magnetized state and drives the fluid toward short-wavelength spin textures. To test this ascription, we reexamine the behavior of spin helices in condensates in which the dipolar interaction is tempered using a rapid sequence of rf pulses. The suppression of the modulated phase observed in this case confirms the crucial role of dipolar interactions.

For this work, spin-polarized ^{87}Rb condensates of up to $2.3(1) \times 10^6$ atoms in the $|F = 1, m_F = -1\rangle$ hyperfine state and at a kinetic temperature of $T \simeq 50$ nK were confined in a single-beam optical dipole trap characterized by trap frequencies $(\omega_x, \omega_y, \omega_z) = 2\pi(39, 440, 4.2)$ s^{-1}. The Thomas-Fermi condensate radius in the $\hat{y}$ (vertical) direction ($r_y = 1.8$ μm) was less than the spin healing length $\xi_S = (8\pi\Delta a n_0)^{-1/2} = 2.4$ μm, where $n_0 = 2.3 \times 10^{14}$ cm^{-3} is the peak density of the condensate. This yields a spinor gas that is effectively two-dimensional with regard to spin dynamics.

The condensate was transversely magnetized by applying a $\pi/2$ rf pulse in the presence of an ambient magnetic field of $B_0 = 165(5)$ mG aligned to the $\hat{z}$ axis. Stray magnetic gradients (curvatures) were canceled to less than 0.14 mG/cm (4.3 mG/cm^2). A helical spin texture was then prepared by applying a transient magnetic field gradient dB_z/dz for a period $\tau_p = 5$–8 ms. Larmor precession of the atomic spins in this inhomogeneous field resulted in a spatial spin texture with a local dimensionless spin of $\mathbf{F} = \cos(\kappa z + \omega_L t)\hat{x} + \sin(\kappa z + \omega_L t)\hat{y}$, where $\vec{\kappa} = (g_F \mu_B/\hbar)(dB_z/dz)\tau_p \hat{z}$ is the helix wave vector. The

fast time variation at the $\omega_L/2\pi \simeq 115$ kHz Larmor precession frequency will be henceforth ignored by considering the spin at a particular instant in this rapid evolution. The helix pitch $\lambda = 2\pi/\kappa$ ranged between 50 and 150 μm. Given $\lambda \gg \xi_S$, the kinetic energy per atom in this spin texture, $E_\kappa = \hbar^2\kappa^2/4m$, was always negligible compared to the ferromagnetic contact-interaction energy [21].

The helical spin texture was then allowed to evolve in a homogenous magnetic field for a variable time before the vector magnetization was measured using a sequence of nondestructive phase contrast images. Because of Larmor precession, a sequence of images taken with circularly polarized light propagating along the $\hat{y}$ direction can be analyzed to determine the column-integrated magnetization perpendicular to the ambient field [22,23], with vector components $\tilde{M}_{x,y} = (g_F\mu_B)\tilde{n}F_{x,y}$, where $\tilde{n}$ the column number density. Subsequent to this imaging sequence, a $\pi/2$ pulse was applied to rotate the longitudinal spin F_z into the transverse spin plane, and a second sequence of images was obtained. A least-squares algorithm comparing data from the two imaging sequences allowed the longitudinal magnetization $\tilde{M}_z$ to be determined [24].

The evolution of helical textures is portrayed in Fig. 1. While uniform spin textures ($\lambda \gg 2r_z$) remain homogenous for long times, helical textures ($\lambda < 2r_z$) spontaneously develop short-wavelength modulations of the magnetization. This modulated phase is characterized by spin domains with typical dimensions of $\simeq 10$ μm, much smaller than the pitch of the imprinted helix, with the magnetization varying sharply between adjacent domains.

To quantify this behavior, we considered the power spectrum of the spatial Fourier transform of the vector magnetization, $|\tilde{\mathbf{M}}(k_x, k_z)|^2$, where (k_x, k_z) is the spatial wave vector in the image plane. This spectrum was found to consist of two distinct components: a central component that quantifies the long-range order of the helical texture,

and a second concentration of spectral power at a discrete set of wave vectors of magnitude $k_{\mathrm{mod}} \simeq 2\pi/(10 \ \mu\mathrm{m})$ representing the short-range order of the final modulated texture. After subtracting out the background representing image noise, we divided spatial Fourier space into regions indicated in Fig. 2 and defined the integrated spectral power in the central region (annular region) as the parametrization of long-range (short-range) spatial order in the quantum fluid.

The formation of the spontaneously modulated texture is reflected in the reduction of the long-range order parameter and the concomitant rise of the short-range order parameter (Fig. 3). During this process, the total spectral power was found to be roughly constant indicating that the bulk of the quantum fluid remains fully magnetized even as the long-range order is reduced. Further, the longitudinal magnetization $\tilde{M}_z$ was found to be much smaller than $\tilde{M}_{x,y}$ throughout this process. The growth rate γ of the short-range order parameter determined from such data was found to rise monotonically with the wave vector κ of the initial helical texture. While the long-range order was found to decrease after sufficiently long evolution times even in condensates prepared with nearly uniform magnetization, we note that stray magnetic field inhomogeneities of ~ 5 μG across the axial length of the condensate would by themselves produce a helical winding across the condensate over a period of 300 ms, constraining our ability to test the stability of homogenous spin textures.

Another measure of the spontaneous short-range modulation in the condensate is the appearance of polar-core spin vortices throughout the gas. Such vortices were identified as in Ref. [18] by a net winding of the transverse magnetization along a closed two-dimensional path of nonzero magnetization in the imaged gas. The number of identified spin vortices was roughly proportional to the short-range order parameter, with no vortices identified in the initially prepared spin helix and up to 6 vortices/
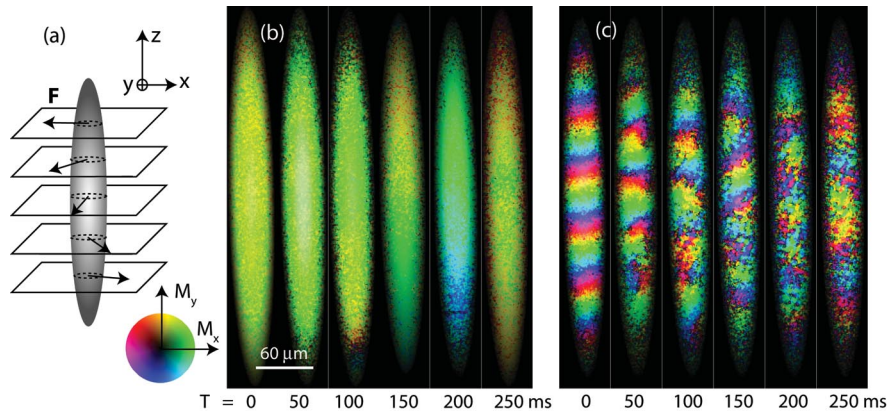

FIG. 1 (color).   Spontaneous dissolution of helical textures in a quantum degenerate ^{87}Rb spinor Bose gas. A transient magnetic field gradient is used to prepare transversely magnetized (b) uniform or (a),(c) helical magnetization textures. The transverse magnetization column density after a variable time T of free evolution is shown in the imaged x-z plane, with orientation indicated by hue and amplitude by brightness (color wheel shown). (b) A uniform texture remains homogeneous for long evolution times, while (c) a helical texture with pitch $\lambda = 60$ μm dissolves over ~ 200 ms, evolving into a sharply spatially modulated texture.
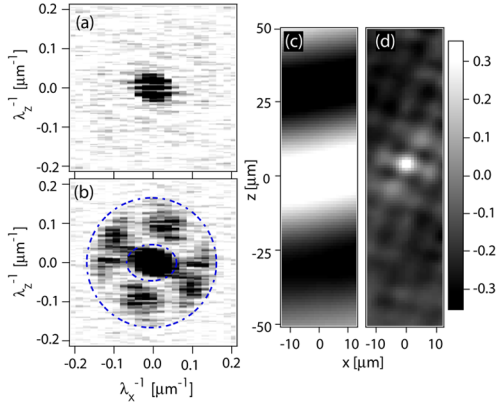
FIG. 2 (color online).   Power spectrum of the spatial Fourier transform and the two-point correlation function $G(x, z)$ for the initial spin helix (a),(c) and the spontaneously modulated phase (b),(d). These data are derived from the same image sequence shown in Fig. 1(c). The images (a),(c) correspond to an evolution time $T = 0$ ms while (b),(d) correspond to an evolution time $T = 250$ ms. The short-range spatial order is defined as the integrated spectral power in the annular region shown in (b).

image identified in the strongly modulated texture produced after free evolution. In each instance, the number of vortices with positive and negative charge was found to be approximately equal.

A striking feature in the evolution of spin textures is the significant rise in the kinetic energy of the condensed atoms, reaching a value of $\hbar^2 k_{mod}^2/8m = h \times 6$ Hz per atom given that roughly half the spectral weight of the texture's magnetization is at the wave vector k_{mod}. One expects the total energy per atom in the condensate to be constant during this evolution, or even to diminish through the transfer of energy to the noncondensed portion of the
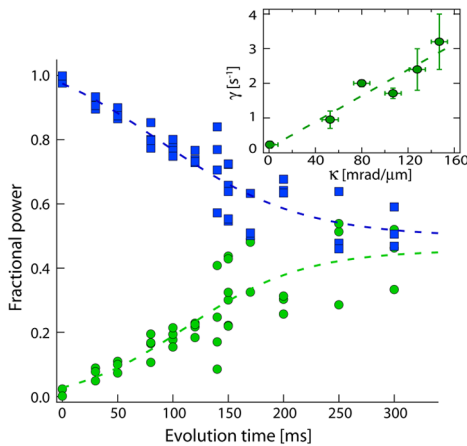

FIG. 3 (color online).   Growth of the spontaneously modulated phase (●) coincides with a reduction in the integrated energy in the low spatial frequency region (■). The data shown correspond to an initial helical pitch of 60 μm. Inset: The initial growth rate γ of the modulated phase as a function of the helix wave vector. These were extracted from linear fits of the short-range order parameter at short evolution times.

gas. Yet, in examining the energy of the initially prepared spin helix, we find the local contact-interaction energy is minimized, the quadratic Zeeman energy is just $q/2 = h \times 1$ Hz at the ambient magnetic field, and the kinetic energy of the spin helix is just $E_\kappa < h \times 0.5$ Hz for a helix pitch of $\lambda > 50$ μm.

This apparent energetic deficit of the spin helix state can be accounted for by the magnetic dipole interaction. The on-axis magnetic field produced by a spin helix in an infinite axial column of gas with a Gaussian transverse density profile can be simply calculated. From this calculation, we estimate that a gas with uniform transverse magnetization possesses an excess of $E_d = \mu_0 g_F^2 \mu_B^2 n_0/2 \sim h \times 5$ Hz compared to the energy of a tightly wound helix, a figure that is close to the excess kinetic energy of the finely modulated texture.

To confirm the role of magnetic dipolar interactions in the evolution of these spin textures, we employed a modification of the NMR technique of spin-flip narrowing [25] to eliminate effectively the dipolar interactions. The interaction energy of two magnetic dipoles separated by the displacement vector $\mathbf{r}$ is proportional to $\mathbf{F}_1 \cdot \mathbf{F}_2 - 3(\hat{r} \cdot \mathbf{F}_1)(\hat{r} \cdot \mathbf{F}_2)$. If both dipoles experience rapid, common spin rotations that evenly sample the entire $SO(3)$ group of rotations, the interaction energy will average to zero regardless of the relative orientations of the spin vectors $\mathbf{F}_{1,2}$ and of the displacement vector $\mathbf{r}$. We note that such spin rotations also annul the quadratic Zeeman shift. However, since the nature of the spontaneously modulated phase was observed to be unchanged as q was varied over a factor of 5 ($0.8 < q/h < 4$ Hz), we suggest this annulment is inconsequential.

Experimentally, after the initial spin texture had been prepared as before, we effected such spin rotations by applying a rapid sequence of $\pi/2$ rf pulses to the Larmor precessing atoms at random intervals, and thus, along random rotation axes, at a mean rate of 1–2 kHz. We confirmed that such a sequence of $\pi/2$ pulses led to an uniform sampling of the rotation group and that each pulse was spatially homogenous across the extent of the condensate. The spin helix was allowed to evolve under the constant action of these dipole-cancellation pulses until the pulses ceased and the sample was imaged as described earlier. In this case, the short-range order parameter grew at a similar rate at early evolution times, but reached a lower plateau at late times, demonstrating a suppression of the modulated phase (Fig. 4). The reduction of the excess kinetic energy of the final spin texture in the spin-rotation-averaged sample supports our identification of the dipole energy as its source.

To account for the residual (but weakened) appearance of short-length scale features in the power spectra [Fig. 4(b)], we note that this technique of spin-flip narrowing is most effective in the case of static dipoles. It is possible that motion of the gas, either coherent or thermal, prevents the $\pi/2$ pulse train from completely eliminating
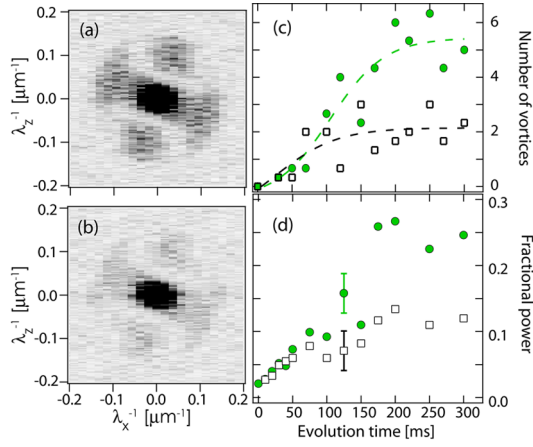
FIG. 4 (color online). Spatial power spectra (a) without or (b) with the application of rapid rf pulses during the 200 ms evolution following the preparation of the helical spin texture, are averaged over four experimental repetitions. Eliminating the dipolar interactions suppresses the short-range spatial modulation of the final spin texture. (c) The average number of detected spin vortices and (d) the short-range order parameter are shown vs evolution time. Square symbols indicate data obtained when the dipolar interaction is spatially averaged. In all cases, the initial helical pitch was $\lambda = 80$ μm.

dipolar interactions. The suppression of the modulated phase was less evident for large helix wave vectors ($\kappa > 110$ mrad/μm), presumably due to the faster growth of the spontaneously modulated phase. Further, we note that recent predictions of nondipolar instabilities in helical textures [26] do not apply for our experimental conditions ($1 < q/h < 4$ Hz, $0 < \kappa < 0.15$ μm^{-1}).

Finally, we note the presence of distinct features in the spatial Fourier spectrum of the spontaneously modulated phase [Fig. 2(b)]. The interpretation of these features is aided by considering the spatial correlation function of the magnetization, which we define as

$$G(\delta \mathbf{r}) = \frac{\sum_{\mathbf{r}} \tilde{\mathbf{M}}(\mathbf{r} + \delta \mathbf{r}) \cdot \tilde{\mathbf{M}}(\mathbf{r})}{(g_F \mu_B)^2 \sum_{\mathbf{r}} \tilde{n}(\mathbf{r} + \delta \mathbf{r}) \tilde{n}(\mathbf{r})}. \quad (1)$$

For the initial spin helix, this correlation function shows the long-range sinusoidal variation of the transverse magnetization at the corresponding pitch. In contrast, the final texture shows significant short-range correlations in both the $\hat{x}$ and $\hat{z}$ directions, with regions of opposite alignment arranged in the form of a checkerboard with a lattice spacing $l_m \simeq 10$ μm [Fig. 2(d)]. While these correlations are strongest at short range, they persist, albeit with diminished strength, even for separations $\delta r \gg l_m$. This lattice structure is suppressed in helices evolving under the active cancellation of dipolar interactions.

In conclusion, we observe a magnetic-dipole-mediated instability resulting in the emergence of spontaneously ordered spin domains in a quantum degenerate spinor Bose gas. The demonstration of the significance of magnetic dipolar interactions in a ^{87}Rb spinor gas presents a

new arena for the study of dipolar quantum gases. Of particular interest is the influence of such anisotropic interactions on the true ground state of these spinor gases and the question of whether this self-organized modulated spin texture represents an unforeseen equilibrium phase of this dipolar quantum fluid.

[1] M. C. Cross and P. C. Hohenberg, Rev. Mod. Phys. **65**, 851 (1993).
[2] M. Seul and D. Andelman, Science **267**, 476 (1995).
[3] T. Garel and S. Doniach, Phys. Rev. B **26**, 325 (1982).
[4] *Ferrofluids: Magnetically Controllable Fluids and Their Applications*, edited by S. Odenbach, Lecture Notes in Physics Vol. 594 (Springer, New York, 2002).
[5] K. De'Bell, A. B. MacIsaac, and J. P. Whitehead, Rev. Mod. Phys. **72**, 225 (2000).
[6] E. Dagotto, Science **309**, 257 (2005).
[7] *Quantum Magnetism*, edited by U. Schollwöck *et al.*, Lecture Notes in Physics Vol. 645 (Springer, Berlin, 2004).
[8] D. Jaksch *et al.*, Phys. Rev. Lett. **85**, 2208 (2000).
[9] A. Micheli, G. K. Brennan, and P. Zoller, Nature Phys. **2**, 341 (2006).
[10] K. Góral, L. Santos, and M. Lewenstein, Phys. Rev. Lett. **88**, 170406 (2002).
[11] H. P. Büchler *et al.*, Phys. Rev. Lett. **98**, 060404 (2007).
[12] J. Stuhler *et al.*, Phys. Rev. Lett. **95**, 150406 (2005); T. Lahaye *et al.*, Nature (London) **448**, 672 (2007).
[13] J. Doyle *et al.*, Eur. Phys. J. D **31**, 149 (2004).
[14] T. L. Ho, Phys. Rev. Lett. **81**, 742 (1998); T. Ohmi and K. Machida, J. Phys. Soc. Jpn. **67**, 1822 (1998).
[15] J. Stenger *et al.*, Nature (London) **396**, 345 (1998).
[16] M.-S. Chang *et al.*, Nature Phys. **1**, 111 (2005).
[17] J. Kronjager *et al.*, Phys. Rev. Lett. **97**, 110404 (2006).
[18] L. Sadler *et al.*, Nature (London) **443**, 312 (2006).
[19] L. Santos, G. Shlyapnikov, and M. Lewenstein, Phys. Rev. Lett. **90**, 250403 (2003).
[20] S. Yi and H. Pu, Phys. Rev. Lett. **97**, 020401 (2006); Y. Kawaguchi *et al.*, Phys. Rev. Lett. **97**, 130404 (2006).
[21] In a transversely magnetized spin texture in an $F = 1$ spinor condensate, only half of the atoms, those in the $m_F = \pm 1$ magnetic sublevels, acquire kinetic energy.
[22] M. Vengalattore *et al.*, Phys. Rev. Lett. **98**, 200801 (2007).
[23] J. M. Higbie *et al.*, Phys. Rev. Lett. **95**, 050401 (2005).
[24] Further details on the imaging system and signal analysis will be discussed elsewhere.
[25] C. Slichter, *Principles of Magnetic Resonance* (Springer, New York, 1978).
[26] A. Lamacraft, arXiv:0710.1848; R. W. Cherng *et al.*, arXiv:0710.2499.